

valid at low vapor pressures. The surface contour calculated by Kontorovich is a nonequilibrium state which is detectable only in the limit of vanishing vapor.

We gratefully acknowledge helpful conversations with K. de Conde, D. Goodstein, S. Ma, S. Putterman, F. Reif, I. Rudnick, and T. M. Sanders. We thank P. L. Richards for the generous loan of his capacitance bridge.

*Work supported by the National Science Foundation.

¹V. M. Kontorovich, Zh. Eksp. Teor. Fiz. **30**, 805 (1956) [Sov. Phys. JETP **3**, 770 (1956)].

²P. W. F. Gribbon and L. C. Jackson, Can. J. Phys. **41**, 1047 (1963).

³K. A. Pickar and K. R. Atkins, Phys. Rev. **178**, 389 (1969).

⁴W. E. Keller, Phys. Rev. Lett. **24**, 569 (1970).

⁵E. R. Huggins, Phys. Rev. Lett. **24**, 573 (1970).

⁶D. L. Goodstein and P. G. Saffman, Proc. Roy. Soc., Ser. A **325**, 447 (1971).

⁷S. J. Putterman and I. Rudnick, Phys. Today **24**, No. 8, 39 (1971).

⁸R. de Bruyn Ouboter, J. Low Temp. Phys. **12**, 3

(1973).

⁹E. Van Spronsen, H. J. Verbeek, R. de Bruyn Ouboter, K. W. Taconis, and H. Van Beelen, Phys. Lett. **45A**, 49 (1973).

¹⁰C. E. Chase, E. Maxwell, and W. E. Millett, Physica (Utrecht) **27**, 1129 (1961).

¹¹W. E. Keller and E. F. Hammel, Phys. Rev. Lett. **17**, 998 (1966).

¹²Taking into account the excess flux of atoms striking the thinned-film surface, we calculate a characteristic time to reach a steady-state thickness,

$$\tau = (\rho_l d_0 / 3\gamma \rho_v g z) (2\pi kT/m)^{1/2},$$

where γ is the accommodation coefficient, ρ_l is the liquid density, ρ_v is the vapor density, k is Boltzmann's constant, and m is the mass of a helium atom. At $T = 1.0^\circ\text{K}$, $\tau \approx 1$ sec.

¹³Presumably this would also apply to a recent calculation of the free surface near a vortex line by K. C. Harvey and A. L. Fetter, J. Low Temp. Phys. **11**, 473 (1973).

¹⁴A. Bianconi and B. Maraviglia, J. Low Temp. Phys. **1**, 201 (1969).

¹⁵This point was brought to our attention by Professor T. M. Sanders.

¹⁶F. Wagner, J. Low Temp. Phys. **13**, 185 (1973).

Amplitudes and Level Spacings of Bound States in Superconducting Cd†

S. L. Colucci, W. J. Tomasch, and Hyung Joon Lee

Department of Physics, University of Notre Dame, Notre Dame, Indiana 46556

(Received 28 January 1974)

Bound- and virtual-state structure has been observed in the tunneling characteristics of thick Cd films deposited over Pb. We observed amplitude effects displaying a temperature dependence not previously reported. An important point is made concerning basic spacings of bound and virtual levels. Amplitudes and level spacings appear to contain retrievable proximity-effect information. Taking nonlinear effects into account, a value of $v_F = 1.30 \times 10^8$ cm/sec is obtained for the c direction.

Oscillatory structure in the tunneling density of states $\rho_S(\omega)$ of thick ($d_1 \approx 1 \mu\text{m}$) superconducting films (M_1) results from interference between degenerate quasiparticle states coupled by a pairing-potential perturbation ($\delta\Delta = \Delta_2 - \Delta_1$) due to the proximity of a thinner second metal (M_2).¹⁻⁷ This Letter deals with the case in which M_2 is a superconductor with energy gap $2\Delta_2 \gg 2\Delta_1 \geq 0$. A quasiparticle wave incident upon the interface M_1/M_2 suffers partial reflection when it has energy $\omega > \Delta_2$ and total reflection when $\omega < \Delta_2$ (no states available in M_2). In either event, interference produces standing-wave resonances associated with energies $\omega = \omega_n$. For sufficiently long mean free paths $l_1 = d_1/\gamma$, resonances contribute

peaks to ρ_S corresponding to bound-state ($\omega < \Delta_2$) and virtual-state ($\omega > \Delta_2$) levels. For $\gamma \gg 1$, a reasonably detailed theory due to Wolfram⁵ predicts an average level separation $\langle \delta\omega \rangle \approx hv_F/2d_1$, where v_F is the renormalized Fermi velocity. This is the same result as for virtual states when $\delta\Delta < 0$ and $\gamma \sim 1$.^{3,5,6} Leaving this limit, however, Wolfram predicts a strong harmonic contribution which adds a second series of peaks ($\omega < \Delta_2$, $\omega > \Delta_2$), so that $\langle \delta\omega \rangle \approx hv_F/4d_1$.

Early attempts to observe bound levels ($\Delta_1 > 0$) employed In (M_1) and Pb (M_2).⁷ These yielded very weak structure, possibly because of interdiffusion of In and Pb. In at least one instance, however, stronger structure was observed re-

sembling that generally associated with quasi-particle resonances. Structure was confined to biases (V) corresponding to $\omega < \Delta_2$ and exhibited an average bias spacing $\langle \delta V \rangle$ satisfying $e\langle \delta V \rangle \approx \hbar v_F/4d_1$. Because of experimental uncertainties, this result could at best be considered suggestive. Very strong bound-state structure has been reported recently by Rowell for Zn (M_1) over Pb (M_2),^{8,9} level spacings being interpreted in terms of $\hbar v_F/2d_1$. We wish to report somewhat weaker bound-state structure for Cd over Pb, structure exhibiting a temperature dependence not reported previously. Our results support the view that $\langle \delta \omega \rangle \approx \hbar v_F/4d_1$ for Cd, and quite possibly for Zn as well. They also indicate that relative amplitudes and nonlinear peak spacings contain retrievable information concerning the spatial and temperature dependence of Δ_1 and Δ_2 .

Strips of Pb ($d_2 \approx 0.3 \mu\text{m}$) evaporated onto glass substrates ($\sim 77 \text{ K}$) were promptly covered with $3\text{--}6 \mu\text{m}$ of Cd [$(3\text{--}9) \times 10^{-7} \text{ Torr}$] to form one side of a tunnel junction. Films were later exposed to air and their edges painted with Formvar. Pb counter electrodes were then evaporated over the natural oxide barrier. Derivatives $V'(V) = dV/dI$ and $V''(V) = d^2V/dI^2$ were measured by the usual ac method, junctions typically exhibiting ratios $V'(0)/(V')_{\text{max}} \approx 100$ at 0.3 K . Film thicknesses were measured with a Michelson interferometer. X-ray studies indicate strong c -axis texture in these Cd films.

Maximum excess currents are anticipated for biases V_n which align the counter-electrode gap edge (at Δ_{CE}) with peaks in ρ_S , each maximum corresponding to a peak in V'' .¹⁰ Data for two junctions (A and B) are presented in Fig. 1, peaks in V'' having been indexed consecutively ($\Delta_1 + \Delta_{CE} < V_1 < V_2 < \text{etc.}$). For now, peaks above $V_0 = \Delta_{CE} + \Delta_2 \approx 2\Delta(\text{Pb}) \approx 2.8 \text{ mV}$ will be taken to represent virtual-state structure. Junction A exhibits stronger structure ($\sim 11\%$ in the ac conductance at 1 K) than B ($1\text{--}2\%$).¹¹ The Cd film of A is also thinner ($d_1 = 3.9 \mu\text{m}$) than that of B ($5.7 \mu\text{m}$). These films display marked proximity effects above $T_c(\text{bulk}) = 0.54 \text{ K}$, A exhibiting well-developed gap structure in $I(V)$ by 1.0 K ($\Delta_1 \approx 0.07 \text{ meV}$), B showing definite signs of gap structure at 0.9 K . At 0.28 K , A and B yield values $2\Delta_1$ in the range $0.15\text{--}0.19 \text{ meV}$.

Except for peak $2A$, an even-indexed peak at V_n is never weaker than its neighbor at V_{n+1} provided $1 \leq T \leq 4.2 \text{ K}$. Peak $2A$ is $\sim 9\%$ stronger than $3A$ at 4.2 K , but by 1 K , its amplitude is already as in Fig. 1 (0.28 K). Unlike A , lowering B be-

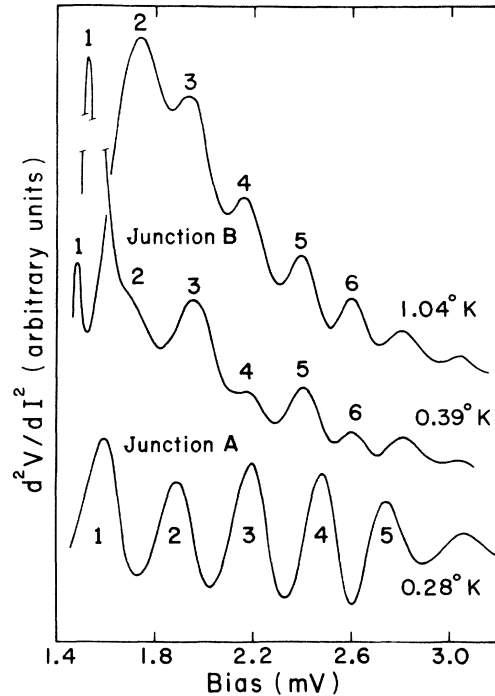


FIG. 1. Second derivative data $V'' = d^2V/dI^2$ for two junctions exhibiting limiting types of behavior. Numbered peaks correspond to bound-state levels. Based on ac conductance, A exhibits structure 6–10 times as strong as B . Peaks $2B$, $4B$, and $6B$ become systematically weaker upon lowering T from 1.04 to 0.39 K . For A , all amplitudes remain unchanged between 1.0 and 0.28 K .

low 1 K produces dramatic amplitude effects (Fig. 1). Peak $2B$, prominent at 1.04 K , virtually disappears by 0.39 K , while $1B$ and $3B$ become stronger. All even-indexed peaks ($2B, 4B, 6B$) are significantly weaker at 0.39 K , the effect being less pronounced at higher V . Lowering T to 0.28 K produces no further change. Amplitude effects are not confined to bound levels. Weak even-indexed peaks $\omega > 2.8 \text{ mV}$ always accompany weak even-indexed peaks $\omega < 2.8 \text{ mV}$, and vice versa. A , B , and a junction of intermediate behavior (C) all yield very similar values of $e\langle \delta V \rangle \times 4d_1/\hbar$. Temperature effects will be interpreted in terms of the reasonable assumption that strong (weak) structure in ρ_S produces strong (weak) structure in V'' . To this end we now examine the properties of $\rho_S(\omega)$ as given by Eq. (24) of Ref. 5.

Four parameters ($\Delta_1, \Delta_2, \gamma, c = 4d_1/\hbar v_F$) completely specify $\rho_S(\omega)$ in terms of $\rho_N = m^*/\pi\hbar^2\tilde{k}_F$ ($\tilde{k}_F \approx k_F$).⁵ It is enlightening to examine the behavior of ρ_S under simplifying conditions. For $\gamma \ll 1$, $\rho_S(\omega)$ exhibits sharp peaks with maxima

at energies ($\Delta_1 < \omega_n < \Delta_2$) satisfying¹²

$$\tan(\pi c \Omega_1) = -\Omega_1 W_2 / (\Delta_1 \Delta_2 - \omega^2), \quad (1)$$

where $\Omega_1 = (\omega^2 - \Delta_1^2)^{1/2}$ and $W_2 = (\Delta_2^2 - \omega^2)^{1/2}$. For these energies ω_n , ρ_S is given in terms of $\rho_0 = \rho_N \omega / \Omega_1$ by

$$\rho_S = \rho_0 \gamma^{-1} [1 + (-1)^{n+1} \Delta_1 / \omega]. \quad (2)$$

Equation (1) has at least one solution, $\omega_1 > \Delta_1$, even for $c(\Delta_2 - \Delta_1) \ll 1$. Additional solutions oc-

cur ($\Delta_1 < \omega_1 < \omega_2 < \dots < \Delta_2$) as c is increased by increasing d_1 . Peaks are not uniformly spaced and $\langle \delta \omega \rangle$ is commonly $\sim 10\%$ smaller than $c^{-1} = \hbar v_F / 4d_1$. Amplitude effects are easily understood in the limit of Eq. (2). The factor $(-1)^{n+1}$ alternately strengthens and weakens peaks depending on whether n is odd or even, the effect being less pronounced for higher ω_n .

Amplitude effects persist to large values of γ ($\sinh^2 \gamma \gg 1$), $\rho_S(\omega)$ exhibiting broad levels corresponding to

$$\rho_S - \rho_0 \cong 2\rho_0 e^{-\gamma} [- (\Delta_1 / \omega) \cos \varphi(\omega) + e^{-\gamma} \cos 2\varphi(\omega)]. \quad (3)$$

Maxima are contributed near $\varphi = n\pi$ ($n=1, 3$, etc.) by $-\cos \varphi$, and near $\varphi = n\pi$ ($n=1, 2, 3$, etc.) by $\cos 2\varphi$. The approximate periods of these terms are $\hbar v_F / 2d_1$ and $\hbar v_F / 4d_1$, respectively. For $\Delta_1 / \omega \sim e^{-\gamma}$, interference again alternately strengthens and weakens peaks depending on whether n is odd or even, the effect being less pronounced for larger ω . In Eq. (2), relative amplitudes are controlled by Δ_1 / ω , while in Eq. (3), γ also plays a role. For n and γ fixed, the influence of Δ_1 / ω can be reduced either by decreasing Δ_1 (increasing T) or by increasing ω_n (decreasing d_1). Overall amplitudes are controlled by γ . Comparing experiment with theory involves some interpretation since the latter assumes Δ_1 and Δ_2 are constant over d_1 and d_2 , whereas proximity phenomena cause Δ_1 and Δ_2 to vary. We assume Δ_1 corresponds to a suitable average over d_1 , and Δ_2 to a somewhat depressed value appropriate for M_1 / M_2 .

Figure 2 presents plots (I, II, III) of $\rho_S(\omega) / \rho_N$ computed from Eq. (24) of Ref. 5 employing parameters suitable for A and B. Making allowances for background, one notes a general resemblance to corresponding curves of Fig. 1. Locations of maxima in V'' , $E_n = eV_n - \Delta_{CE}$, are also indicated. Values of Δ_{CE} employed are appropriate for Pb and compatible with $I(V)$. Considerations involved in selecting specific parameter values for ρ_S demonstrate the interplay between peak locations and amplitudes. Peaks not too near Δ_1 or Δ_2 are least sensitive to Δ_1 and Δ_2 , and hence permit an initial estimate of c . Fits to E_1 and E_2 can then be improved via Δ_1 . (Increasing Δ_1 raises low-lying peaks to higher ω even though d_1 remains constant.) Changing Δ_1 may also cause marked amplitude effects (III \rightarrow II). Spacings and relative amplitudes near $\omega = \Delta_2$ depend on Δ_2 . For I, relative amplitudes of 4 and 5 fix Δ_2 to within $\pm 2\%$. Values of Δ_2 obtained

are smaller than $\Delta(\text{Pb}) = 1.39$ meV and consistent with $V_0 \approx 2.8$ mV. All peaks ($\omega < \Delta_2$) become sharp spikes for $\gamma \leq 0.5$, while all even peaks become very weak for $\gamma \geq 4$. Larger γ may also cause

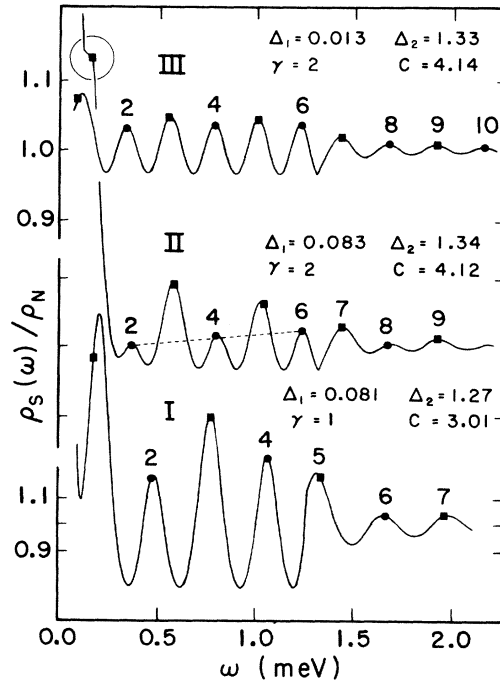


FIG. 2. Computed density of states versus energy (ω). Parameters are appropriate for corresponding curves of Fig. 1. Locations of peaks in V'' are indicated by dots placed on computed curves to facilitate comparisons. The dashed line draws attention to strengthening of even-indexed peaks with increasing ω , a signature characteristic of both experiment and theory. Levels are not uniformly spaced near $\omega = \Delta_1$ and $\omega = \Delta_2$. Curve III differs little from that obtained with $\Delta_1 = 0$. The first peak (ρ_S) of II (top left, encircled) has been exaggerated for visibility. Values of Δ_{CE} employed for I, II, and III are 1.42, 1.35, and 1.36 meV, respectively.

resolution problems (circle, Fig. 2). Initial parameters may be readjusted to improve overall fit. Typical changes of c during this process amount to 1–2%. Since c is not very sensitive to changes in γ , values employed ($\gamma=1, 2$) are rather approximate and probably do not represent the best overall fit.

For B , peak locations and relative amplitudes are accounted for satisfactorily provided Δ_1 increases from about 0.01 to 0.08 meV between 1.04 and 0.39 K. A has not been fitted quite as well, peaks 3 and 4 being of different height. For $\Delta_1=0$, odd and even peaks are of equal strength. Observed weakening of peak 2A is presumably caused by the increase of Δ_1 (averaged over d_1) as T is decreased from 4.2 K. Observed proximity effects in A and B appear to qualitatively support these interpretations. Based on thickness measurements of three Cd films (A, B, C), we obtain $v_F = 1.30 \times 10^8$ cm/sec ($\pm 3\%$ scatter), to be compared with 1.27×10^8 cm/sec obtained by Rahn, Sabo, and Weir¹³ from magnetic surface-state (MSS) studies.

Zn tunneling results also appear to exhibit a weakening of alternate conductance peaks.⁹ Since our interpretation would resolve the factor-of-2 disagreement between tunneling^{8,9} and MSS¹⁴ determinations of v_F (Zn, c axis), one wonders if the scattering argument of Ref. 8 (for M_1 superconducting) may not need modification. From Eq. (3), relative amplitudes of even-indexed peaks in $\rho_S(\omega)$ are very weak for $e^{-\gamma} \ll 1$. They are also very weak for $\delta\Delta/\Delta_1 \ll 1$, even when $\gamma \ll 1$. Equation (2) then yields $\rho_S \approx (\rho_0/\gamma)\delta\Delta/\Delta_1$ (n even) and $\rho_S \approx 2\rho_0/\gamma$ (n odd), while Eq. (3) yields $\rho_S - \rho_0 \approx 2\rho_0 e^{-\gamma} \cos\varphi$. Hence one can force $\langle\delta\omega\rangle \approx \hbar v_F/2d_1$ by $\delta\Delta/\Delta_1 \ll 1$, or by $\gamma^{-1} \ll 1$. This suggests approximations valid only in these limits may have been employed.⁸ A quasiparticle may suffer repeated scattering encounters with $\delta\Delta$. The simplest process S_1 involves a single encounter³ and yields $\delta\omega = \hbar v_F/2d_1$. The scattering amplitude varies roughly as $e^{-\gamma}\Delta_1\delta\Delta$ ($\omega < \Delta_2$). For M_1 normal ($\Delta_1=0$), another process, S_2 , involving two encounters can be employed,¹⁵ yielding $\delta\omega = \hbar v_F/4d_1$. The scattering amplitude varies roughly as $e^{-2\gamma}(\delta\Delta)^2$ ($\omega < \Delta_2$). Both S_1 and S_2 may be important when $\Delta_1 > 0$, the relative im-

portance of S_2 being measured by $e^{-\gamma}\delta\Delta/\Delta_1$. Hence S_2 may be omitted if $\delta\Delta/\Delta_1$ or γ^{-1} are sufficiently small. For Zn (M_1) over Pb (M_2), $\delta\Delta/\Delta_1 \sim 7$. The generally strong structure observed^{8,9} suggests $e^{-\gamma}\delta\Delta/\Delta_1 \sim 1$ may be reasonable. If so, S_2 cannot be neglected, and $\delta\omega = \hbar v_F/4d_1$ even when M_1 is superconducting. The scattering description now yields a v_F (Zn) similar to that obtainable from our interpretation, except for Wolfram's nonlinear corrections.

A truly critical assessment of the detailed applicability of Wolfram's theory in its present form would require a direct comparison between an experimentally extracted tunneling density of states and $\rho_S(\omega)$. This may well be possible. The advantage of having a theory which treats spatial variations of Δ_1 and Δ_2 in a more nearly self-consistent way seems fairly clear in view of proximity-effect information stored in relative amplitudes and nonlinear level spacings.

The authors wish to thank L. S. Wong for valuable assistance, L. S. Darken for valuable discussions, and G. L. Wells for design and construction of a prototype He³ refrigerator.

†Work supported by the National Science Foundation under Grant No. GH-34519.

¹W. J. Tomasch, Phys. Rev. Lett. **15**, 672 (1965).

²W. J. Tomasch, Phys. Rev. Lett. **16**, 16 (1966).

³W. L. McMillan and P. W. Anderson, Phys. Rev. Lett. **16**, 85 (1966).

⁴W. J. Tomasch and T. Wolfram, Phys. Rev. Lett. **16**, 352 (1966).

⁵T. Wolfram, Phys. Rev. **170**, 481 (1968).

⁶W. L. McMillan, Phys. Rev. **175**, 559 (1968).

⁷W. J. Tomasch, Phys. Lett. **A26**, 379 (1968).

⁸J. M. Rowell, Phys. Rev. Lett. **30**, 167 (1973).

⁹J. M. Rowell, J. Vac. Sci. Technol. **10**, 702 (1973).

¹⁰Peaks in the first and second derivatives are in one-to-one correspondence.

¹¹Junction A exhibits a well-resolved current peak centered at V_2 .

¹²The minus sign in the numerator of Eq. (27) of Ref. 5 is a typographical error.

¹³J. P. Rahn, J. J. Sabo, Jr., and J. E. Weir, Phys. Rev. B **6**, 4406 (1972).

¹⁴J. P. Rahn and J. J. Sabo, Jr., Phys. Rev. B **6**, 3666 (1972).

¹⁵J. M. Rowell and W. L. McMillan, Phys. Rev. Lett. **16**, 453 (1966).